

Beyond and Before the Quadrupole: Eccentricity Enabling the Earliest Warning and Localization of Gravitational Waves with Ground-Based Detectors

Tao Yang^{1,*} Rong-Gen Cai^{2,3,4,†} Zhoujian Cao^{5,4,‡} and Hyung Mok Lee^{1,§}

¹*Center for the Gravitational-Wave Universe, Astronomy Research Center,
Seoul National University, 1 Gwanak-ro, Gwanak-gu, Seoul 08826, Korea*

²*CAS Key Laboratory of Theoretical Physics, Institute of Theoretical Physics,
Chinese Academy of Sciences, Beijing 100190, China*

³*School of Physical Science and Technology, Ningbo University, Ningbo, 315211, China*

⁴*School of Fundamental Physics and Mathematical Sciences, Hangzhou Institute for Advanced Study (HIAS),
University of Chinese Academy of Sciences, Hangzhou 310024, China*

⁵*Department of Astronomy, Beijing Normal University, Beijing 100875, China*

(Dated: October 13, 2023)

The early and precise localization of gravitational waves (GWs) is pivotal in detecting their electromagnetic (EM) counterparts, especially for binary neutron stars (BNS) and neutron star-black hole binaries (NSBH). In this paper, we pioneer the exploration of utilizing the higher harmonic modes induced by the eccentricity of compact binaries to localize GWs with ground-based detectors even before the dominant quadrupole mode enters the detector band. Our theoretical analysis marks a first in proposing a strategy for gaining the earliest possible warning and maximizing preparation time for observing pre- and/or post-merger EM counterparts. We simulate three typical binaries from GWTC-3 with eccentricities ranging from 0.05 to 0.4. Our results reveal that the third-generation (3G) detectors (low frequency cut-off $f_0 = 5$ Hz) can accumulate sufficient signal-to-noise ratios through higher modes before the onset of quadrupole mode entry into the band. Notably, relying solely on the higher modes, the 3G detector network ET+2CE achieves an average localization on the order of $1 - 10^2 \text{ deg}^2$ around 1-1.8 hours before the merger of a GW170817-like BNS, and $10 - 10^3 \text{ deg}^2$ approximately 18-30 minutes prior to the merger of a GW200115-like NSBH. Moreover, in the near face-on orientations which are generally more favorable for EM counterpart detection, the localization can be further improved.

I. INTRODUCTION

Multi-messenger observations of gravitational waves (GWs) and their electromagnetic (EM) counterparts play vital roles in cosmology, astrophysics, and fundamental physics [1–9]. Notably, with the observations of EM counterparts, the host galaxies of GWs and consequently their redshifts can be readily identified, enabling the direct measurement of the Hubble constant through GW standard sirens [3, 10–12]. However, the successful capture of EM counterparts heavily relies on the precise and timely localization of GW sources [13–16]. The early warning and localization of GWs, as well as their implications for multi-messenger observations, have been explored from various perspectives [17–25].

Eccentricity can aid not only in distinguishing between isolated and dynamical binary black hole (BBH) formation scenarios [26–29] but also in improving the parameter estimation (including localization) of GWs [30–34]. In particular, recent studies [35–37] demonstrate that the eccentricity of long inspiraling compact binaries can dramatically enhance the accuracy of distance estimation and source localization by several orders of magnitude with space-based decihertz observatories. On the

other hand, neglecting eccentricity will introduce biases in parameter estimation [38–40]. In current detections, GW190521 has been suggested to favor nonzero eccentricities [41, 42]. These research findings suggest that eccentricity is an indispensable factor to consider in GW detection, data analysis, and practical applications.

One prominent feature of eccentric waveforms is the presence of multiple harmonic modes induced by eccentricity [43–46]. The frequency of each harmonic is given by $f_\ell(t) = \ell F(t)$, where F denotes the orbital frequency of the binary. This results in each mode entering the detector band at a distinct time. Consequently, the higher modes ($\ell > 2$) enter the detector band earlier than the dominant quadrupole mode ($\ell = 2$), affording an extended period for the observation of these higher modes. This is particularly beneficial for ground-based detectors that aim to capture GWs at high frequencies, where the inspiral time is very limited. For instance, consider the binary neutron stars (BNS) GW170817 detected by LIGO as an example. The in-band time of the quadrupole mode from 10 Hz to the merger lasts approximately 17 minutes. However, before the quadrupole mode enters the detector band, the higher modes have already been in band for nearly 20 hours (assuming we account for the higher modes up to $\ell = 10$; note that a larger eccentricity would shorten this period). This extended observation window for the higher modes enables the consideration of Earth’s rotation effects, introducing a Doppler effect that can furnish additional angular infor-

* yangtao.lighink@gmail.com

† cairg@itp.ac.cn

‡ zjcao@bnu.edu.cn

§ hmlee@snu.ac.kr

mation regarding the sources. This raises the following questions that we aim to address in this paper: Can we observe these higher modes before the quadrupole mode becomes observable? More importantly, to what degree of accuracy can we localize GW sources solely based on these higher modes even before the quadrupole mode enters the detector band?

Previous works on the early warning of GWs has focused on the time following the entry of the dominant quadrupole mode into the band. In this paper, for the first time, we shift our focus to the time preceding the quadrupole mode's entry. This means we exclusively rely on the higher modes in the absence of the quadrupole mode. The early detection and localization of the higher modes have several implications. If these higher modes can accumulate a substantial signal-to-noise ratio (SNR) before the quadrupole mode enters the detector band, neglecting them in data analysis could not only degrade the SNR but also introduce potential bias in parameter estimation. Successfully monitoring the higher modes facilitates earlier data analysis and parameter estimation. Notably, localization based on the higher modes, even before the quadrupole becomes observable, allows for the earliest warning of electromagnetic (EM) counterparts, especially in the context of BNS and neutron star-black hole (NSBH) binaries. This grants EM telescopes much more preparation time, enhancing the likelihood of capturing EM counterparts and particularly aiding in the capture of potential pre-merger EM counterparts [47–50]. If there is a high likelihood that most NSBH mergers will involve non-disruptive systems, pre-merger signals might provide the sole avenue for EM observations of these systems.

To address the aforementioned questions, we turn to simulations of typical compact binaries that have detected by LIGO-Virgo-KAGRA collaborations. We select three representative binaries from the GWTC-3 catalog [51]: BNS GW170817, NSBH GW200115, and binary black holes (BBH) GW150914. We use these examples to calculate the SNR and localization, specifically focusing on the time before the quadrupole mode enters the detector band. We consider various detector network scenarios, including the second-generation (2G) advanced LIGO, advanced Virgo, KAGRA, and India-LIGO (HLVKI) networks at their designed sensitivity, the third-generation (3G) detector Einstein Telescope (ET) [52], and the extended network ET+2CE, which combines ET with two cosmic explorer detectors¹. The low-frequency cutoffs for the 2G and 3G detector bands are set at 10 Hz and 5 Hz, respectively. It's worth noting that the lower limit of ET can reach 3 Hz², but in this study, we conservatively assume a uniform lower limit of 5 Hz for all 3G detectors. The 3G detectors offer improved sensitivity and a wider detector band that reaches

lower frequencies, resulting in a significantly longer inspiral time for the higher modes before the quadrupole mode enters the detector band.

II. METHODOLOGY

We adopt the non-spinning, inspiral-only, and frequency-domain EccentricFD waveform approximant provided by the LALSUITE software package [53]. The eccentric waveforms are generated using PyCBC [54]. The waveform can be expressed as the sum of harmonics [44]:

$$\tilde{h}(f) = \sum_{\ell=1}^{10} \tilde{h}_{\ell}(f), \quad (1)$$

where $\tilde{h}_{\ell}(f)$ represents the contribution from the ℓ -th harmonic. We modify LALSUITE to extract each harmonic $\tilde{h}_{\ell}(f)$ separately.

Given the relationship $f_{\ell}(t) = \ell F(t)$, the time associated with a fixed frequency varies for each mode. Accounting for Earth's rotation, the antenna pattern functions $F_{+, \times}$ of the detector become time-dependent. Consequently, it's crucial to handle the antenna pattern function for each mode individually, ensuring accurate representation of their time-varying behavior. To establish the relationship between time and frequency $t(f)$ for eccentric binaries, we use the baseline frequency f_2 as a reference and numerically solve the phase evolution of the eccentric orbits [43]. Then for each mode $\tilde{h}_{\ell}(f)$, the associated response functions are $F_{+, \times}(t)$, with the time $t(f \rightarrow 2f/\ell)$. To assess the contribution of higher modes at a particular time, such as during the period before the quadrupole mode enters the band, each mode in Eq. (1) must be truncated at its respective frequency, which corresponds to the time when the quadrupole starts to enter the band.

We adopt the approach of [35] and employ the Fisher matrix technique for GWs [55] to estimate the uncertainty and covariance of the waveform parameters. The Fisher matrix is defined as $\Gamma_{ij} = (\partial_i h, \partial_j h)$, where $\partial_i h = \partial h / \partial P_i$ and P_i represents a parameter in the waveform (refer to [35] and [37] for details). The inner product is defined as

$$(a, b) = 4 \int_{f_{\min}}^{f_{\max}} \frac{\tilde{a}^*(f) \tilde{b}(f) + \tilde{b}^*(f) \tilde{a}(f)}{2S_n(f)} df, \quad (2)$$

here f_{\min} is the low-frequency cutoff of the detector. Then the SNR is $\rho = (h, h)$. The sky localization error is given by $\Delta\Omega = 2\pi |\sin(\theta)| \sqrt{C_{\theta\theta} C_{\phi\phi} - C_{\theta\phi}^2}$ [56], with the covariance matrix of the parameters as $C_{ij} = (\Gamma^{-1})_{ij}$. We incorporate Gaussian priors $\Gamma_{ii}^p = 1/(\delta P_i)^2$ into the Fisher information matrix, where δP_i represents the maximum permissible variation in the parameter [38, 39, 55, 57]. The Fisher matrix approach, with the

¹ <https://gwic.ligo.org/>

² <https://apps.et-gw.eu/tds/?content=3&r=17196>

incorporation of Gaussian priors, has demonstrated consistency with the more computationally intensive Markov Chain Monte Carlo (MCMC) method [39, 57].

To account for the different locations of the detectors and Earth’s rotation effects, we use a geocentric coordinate system. The positions and orientations of the arms for the 2G detector network HLVKI are detailed in Table I of [32]. However, the exact locations and orientations of the 3G detectors ET and CE have not been finalized. In our study, we assume ET is situated in the Netherlands, while the two CE detectors share the same locations and orientations as LIGO Hanford and Livingston³.

For each typical binary, which includes GW170817-like BNS, GW200115-like NSBH, and GW150914-like BBH, we maintain the component masses (m_1 , m_2), redshift z , and luminosity distance d_L consistent with the values of the actual events⁴. For angular parameters P_{ang} , such as the inclination angle ι , sky location (θ, ϕ) , polarization angle ψ , and longitude of ascending nodes axis β , we generate 1000 random sets from a uniform and isotropic distribution. Given the validated use of this eccentric waveform for initial eccentricities up to 0.4 [44], we consider four discrete initial eccentricities: $e_0 = 0.05$, 0.1, 0.2, and 0.4. It’s important to note that e_0 is defined at $f_0 = 10$ Hz for 2G detectors and $f_0 = 5$ Hz for 3G detectors. Given that eccentricity is roughly inversely proportional to frequency [43], the same eccentricity value in the 3G detector context is more conservative than in the 2G detector scenario. Without loss of generality, we set the coalescence time and phase as $t_c = \phi_c = 0$. In total, we simulate 12,000 events. We then average the results across the 1000 P_{ang} for each typical binary at a given eccentricity.

III. RESULTS

Fig. 1 showcases the average SNR and localization, provided exclusively by the higher modes ($\ell > 2$), just before the quadrupole mode ($\ell = 2$) enters the band. We utilize two averaging strategies: first, by averaging across all 1000 P_{ang} samples, and second, by averaging the P_{ang} samples that meet the condition $|\cos \iota| \geq 0.9$. We define the condition $|\cos \iota| \geq 0.9$ (equivalently, $|\iota| \leq 25^\circ$ or $|180^\circ - \iota| \leq 25^\circ$) as near face-on orientations. These orientations are optimal for achieving both a higher SNR and enhanced localization of the GWs. Furthermore, if we detect the EM counterparts of BNS and NSBH, they are more likely to be observed in near face-on orientations [58–60]. It’s worth noting that the inclination angle of GW170817 was roughly 160° [3, 7, 61].

For the 2G detector network HLVKI, the average SNR from the higher modes, before the quadrupole mode enters the detector band, falls below the threshold ρ_{th} in all cases. Only in near face-on orientations does the average SNR of the higher modes for BNS and BBH with $e_0 = 0.4$ meet the threshold. In contrast, all cases under the ET and ET+2CE scenarios not only surpass the SNR threshold but also achieve values on the order of 10^2 for BNS and BBH. This underscores that the 2G detector network lacks the requisite sensitivity to detect higher harmonic modes before the quadrupole mode enters the detector band. On the other hand, 3G detectors can amass a substantial SNR, enabling the easy detection of these higher modes. A notable observation is that a larger eccentricity corresponds to a higher SNR. This relationship stems from the fact that eccentricity induces the higher modes, and an increased eccentricity amplifies their prominence.

For localization, we discard cases where the average localization exceeds 10^4 deg^2 . In the HLVKI scenario, as expected, the early localization from the higher modes, having an average SNR below ρ_{th} , is substantially poor and carries limited significance. It’s only in the specific instances of BNS and BBH with $e_0 = 0.4$, and when in near face-on orientations, that the higher modes can achieve an average localization around $10^2 - 10^3 \text{ deg}^2$ before the quadrupole mode enters the detector band. However, the landscape changes dramatically with the 3G detectors. Using a single ET, the higher modes of BNS can secure an average localization that varies from 600 deg^2 at $e_0 = 0.05$ to 20 deg^2 at $e_0 = 0.4$, all before the quadrupole mode enters the band. Notably, in near face-on orientations, the localization is further enhanced, achieving an order of magnitude of $\mathcal{O}(1) \text{ deg}^2$ at $e_0 = 0.4$.

The localization of GWs benefits greatly from the triangulation which involves analyzing the time delays and intensity differences of signals received at various detector locations. The inclusion of two CE detectors in conjunction with ET forms a network that can significantly enhance the localization of the higher modes. As depicted in the right panel of Fig. 1, the early localization solely from higher modes in nearly all cases is superior to 10^3 deg^2 . Taking into account 1000 random P_{ang} for BNS, the average localization is 144.8, 34.5, 7.5, and 1.4 deg^2 for e_0 values of 0.05, 0.1, 0.2, and 0.4, respectively. In near face-on orientations, these localizations sharpen further to 38.5, 9.3, 2.0, and 0.34 deg^2 , respectively. For NSBH, the average localization spans from 22.4 to 2477.8 deg^2 across all orientations and refines to a range between 4.4 and 461.4 deg^2 in near face-on orientations. The results for BBH align closely in scale with those of BNS. It’s worth noting that these outcomes are assessed at the times just before the quadrupole mode begins to enter the band ($f_2 = 5 \text{ Hz}$). The specific times vary based on the binary type and their respective eccentricities.

The above results demonstrate that, with the 3G detector network, the higher modes of all three typical eccentric binaries contribute significantly to the SNR and

³ The exact detector location and orientation are not critical for this study and will not affect our results, as we simulate binaries uniformly distributed across the sky, aiming for average results.

⁴ <https://gwosc.org/eventapi/html/GWTC/>

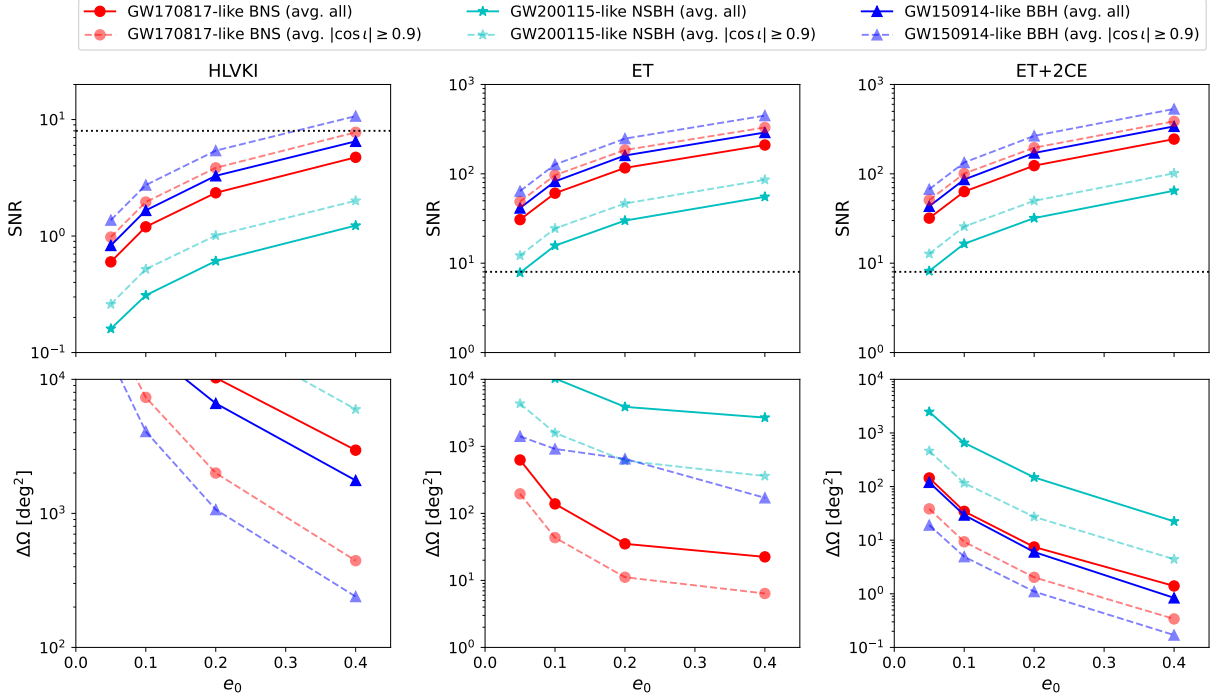


FIG. 1: The average SNR and localization provided exclusively by the higher harmonic modes just before the quadrupole mode enters the band. The solid line represents the average of all 1000 P_{ang} samples, while the dashed line corresponds to the average with $|\cos \iota| \geq 0.9$ (near face-on orientations). The dotted lines in the upper panel indicate the threshold SNR, $\rho_{\text{th}} = 8$. Only cases with $\Delta\Omega < 10^4 \text{ deg}^2$ are shown.

localization even before the dominant quadrupole mode enters the band. To assess how early the higher modes enable us to detect and localize the source, we show the evolution of average SNR and localization against time to merger for the three typical binaries within the ET+2CE network scenario in Fig. 2. We calculate the SNR and localization right before f_2 reaches 15 distinct values ranging from 1.5 to 50 Hz (note the quadrupole mode enters the band at $f_2 = 5 \text{ Hz}$, so the results for this particular point just correspond to the right panel of Fig. 1). We then translate f_2 into the time to merger $t_c - t$, to obtain the evolution of SNR and localization against the time to merger. We place particular emphasis on the period preceding the entry of the quadrupole mode into the band. As illustrated in Fig. 2, in general, a larger eccentricity results in a higher SNR and better localization at a given time. For BNS, with eccentricities ranging from 0.05 to 0.4, the higher modes can achieve the threshold SNR between 4.5 to 7.5 hours prior to the merger. This is notably earlier than the entry of the quadrupole mode into the band. Localization of 100 deg^2 can be achieved around 2-4 hours prior to the merger, derived solely from the higher modes before the quadrupole mode's entry into the band (except for $e_0 = 0.05$, which is slightly after the quadrupole enters the band). In the case of NSBH, the threshold SNR can be obtained 0.5-1.3 hours before the merger. Solely relying on the higher modes, a localization of 100 deg^2 can be achieved 30 minutes before the

merger when $e_0 = 0.4$. The results of BBH are similar to that of BNS, though with a significantly shorter time to merger: 1.3-2.2 minutes for the threshold SNR and 30-50 seconds for a 100 deg^2 localization. In near face-on orientations, the results above can be further improved.

IV. CONCLUSION AND DISCUSSION

In this paper, we aim at checking the idea that whether the higher harmonic modes of eccentric compact binaries can make a significant contribution to the SNR and localization of the sources, even before the dominant quadrupole mode enters the detector band. Unlike the previous studies which focus primarily on the phase when the quadrupole mode is already in-band, our study emphasizes the importance of higher modes before the presence of the quadrupole mode. Consequently, these higher modes could offer the earliest alert and localization, thereby optimizing preparation time for both pre- and post-merger EM counterpart observations.

Our findings reveal that within the 3G detector network ET+2CE scenario, for typical binaries with eccentricities ranging from 0.05 to 0.4, the higher modes alone can achieve a sufficient SNR significantly prior to the quadrupole mode's entry into the detector band. More intriguingly, for a GW170817-like BNS and relying solely on the higher modes, a localization ranging $1 - 10^2 \text{ deg}^2$

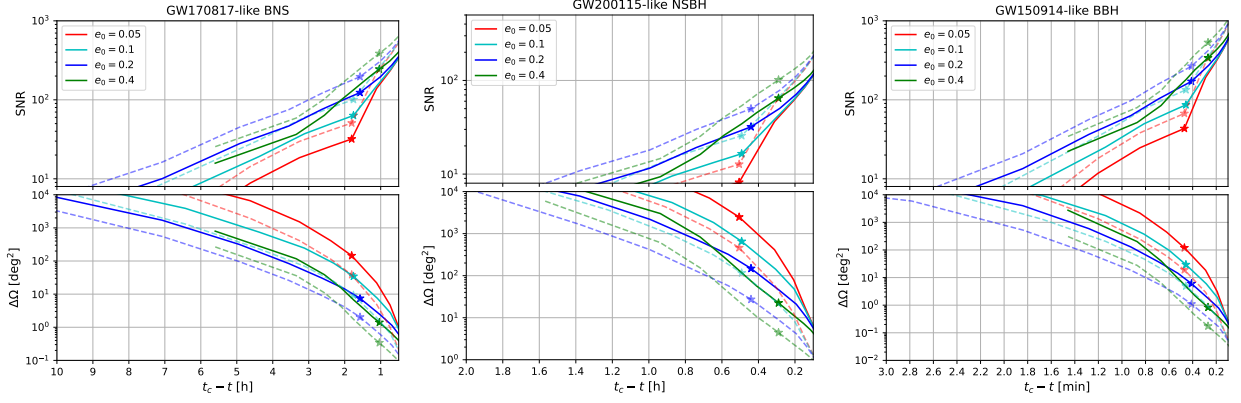


FIG. 2: The average SNR and localization that can be achieved before the time to merger in the ET+2CE scenario. The solid line represents the average of all 1000 P_{ang} samples, while the dashed line corresponds to the average with $|\cos \iota| \geq 0.9$ (near face-on orientations). Stars indicate $f_2 = 5$ Hz, marking the point where the quadrupole mode begins to enter the band.

can be realized approximately 1 to 1.8 hours before the merger. Setting a localization threshold at 100 deg², this can be achieved roughly 2 to 4 hours prior to the merger. Typical NSBH and BBH yield similar results, though with a considerably reduced time to merger. These findings hold significance not only for the EM counterpart observations of BNS and NSBH but also for the potential EM follow-ups of BBH [62–64].

A noteworthy observation in Fig. 1 is that when comparing the ET and ET+2CE scenarios, the addition of two CE detectors doesn’t substantially boost the SNR. This can be ascribed to CE’s reduced sensitivity at lower frequencies in comparison to ET. However, integrating two CE detectors markedly improves GW localization. This underscores that GW localization hinges predominantly on triangulation across multiple detectors, rather than just on SNR.

In this study, we established a conservative low-frequency cut-off for ET at 5 Hz to align with CE. This entails truncating the contributions from all modes below 5 Hz. If we were to expand the observation band to lower frequencies, like 3 Hz or even 1 Hz, higher modes

could enter the band even earlier, potentially yielding more promising results.

ACKNOWLEDGMENTS

This work is supported by the National Research Foundation of Korea NRF-2021R1A2C2012473 and 2021M3F7A1082056. R.G.C is supported by the National Key Research and Development Program of China Grant No. 2020YFC2201502 and 2021YFA0718304 and by National Natural Science Foundation of China Grants No. 11821505, No. 11991052, No. 11947302, No. 12235019. Z.C is supported in part by the National Key Research and Development Program of China Grant No. 2021YFC2203001, in part by the NSFC (No. 11920101003 and No. 12021003), in part by “the Interdiscipline Research Funds of Beijing Normal University” and in part by CAS Project for Young Scientists in Basic Research YSBR-006.

[1] B. P. Abbott *et al.* (LIGO Scientific, Virgo, Fermi GBM, INTEGRAL, IceCube, AstroSat Cadmium Zinc Telluride Imager Team, IPN, Insight-Hxmt, ANTARES, Swift, AGILE Team, 1M2H Team, Dark Energy Camera GW-EM, DES, DLT40, GRAWITA, Fermi-LAT, ATCA, ASKAP, Las Cumbres Observatory Group, OzGrav, DWF (Deeper Wider Faster Program), AST3, CAAS-TRO, VINROUGE, MASTER, J-GEM, GROWTH, JAGWAR, CaltechNRAO, TTU-NRAO, NuSTAR, Pan-STARRS, MAXI Team, TZAC Consortium, KU, Nordic Optical Telescope, ePESSTO, GROND, Texas Tech University, SALT Group, TOROS, BOOTES, MWA, CALET, IKI-GW Follow-up, H.E.S.S., LOFAR, LWA,

HAWC, Pierre Auger, ALMA, Euro VLBI Team, Pi of Sky, Chandra Team at McGill University, DFN, ATLAS Telescopes, High Time Resolution Universe Survey, RIMAS, RATIR, SKA South Africa/MeerKAT), Multi-messenger Observations of a Binary Neutron Star Merger, *Astrophys. J. Lett.* **848**, L12 (2017), [arXiv:1710.05833 \[astro-ph.HE\]](https://arxiv.org/abs/1710.05833).
 [2] B. P. Abbott *et al.* (LIGO Scientific, Virgo, Fermi GBM, INTEGRAL), Gravitational Waves and Gamma-rays from a Binary Neutron Star Merger: GW170817 and GRB 170817A, *Astrophys. J. Lett.* **848**, L13 (2017), [arXiv:1710.05834 \[astro-ph.HE\]](https://arxiv.org/abs/1710.05834).
 [3] B. P. Abbott *et al.* (LIGO Scientific, Virgo, 1M2H,

- Dark Energy Camera GW-E, DES, DLT40, Las Cumbres Observatory, VINROUGE, MASTER), A gravitational-wave standard siren measurement of the Hubble constant, *Nature* **551**, 85 (2017), [arXiv:1710.05835 \[astro-ph.CO\]](#).
- [4] P. Creminelli and F. Vernizzi, Dark Energy after GW170817 and GRB170817A, *Phys. Rev. Lett.* **119**, 251302 (2017), [arXiv:1710.05877 \[astro-ph.CO\]](#).
- [5] J. M. Ezquiaga and M. Zumalacárregui, Dark Energy After GW170817: Dead Ends and the Road Ahead, *Phys. Rev. Lett.* **119**, 251304 (2017), [arXiv:1710.05901 \[astro-ph.CO\]](#).
- [6] T. Baker, E. Bellini, P. G. Ferreira, M. Lagos, J. Noller, and I. Sawicki, Strong constraints on cosmological gravity from GW170817 and GRB 170817A, *Phys. Rev. Lett.* **119**, 251301 (2017), [arXiv:1710.06394 \[astro-ph.CO\]](#).
- [7] K. P. Mooley, A. T. Deller, O. Gottlieb, E. Nakar, G. Hallinan, S. Bourke, D. A. Frail, A. Horesh, A. Corsi, and K. Hotokezaka, Superluminal motion of a relativistic jet in the neutron-star merger GW170817, *Nature* **561**, 355 (2018), [arXiv:1806.09693 \[astro-ph.HE\]](#).
- [8] K. Hotokezaka, E. Nakar, O. Gottlieb, S. Nissanke, K. Masuda, G. Hallinan, K. P. Mooley, and A. T. Deller, A Hubble constant measurement from superluminal motion of the jet in GW170817, *Nature Astron.* **3**, 940 (2019), [arXiv:1806.10596 \[astro-ph.CO\]](#).
- [9] T. Dietrich, M. W. Coughlin, P. T. H. Pang, M. Bulla, J. Heinzel, L. Issa, I. Tews, and S. Antier, Multimes-senger constraints on the neutron-star equation of state and the Hubble constant, *Science* **370**, 1450 (2020), [arXiv:2002.11355 \[astro-ph.HE\]](#).
- [10] D. E. Holz and S. A. Hughes, Using gravitational-wave standard sirens, *Astrophys. J.* **629**, 15 (2005), [arXiv:astro-ph/0504616](#).
- [11] N. Dalal, D. E. Holz, S. A. Hughes, and B. Jain, Short grb and binary black hole standard sirens as a probe of dark energy, *Phys. Rev. D* **74**, 063006 (2006), [arXiv:astro-ph/0601275](#).
- [12] S. Nissanke, D. E. Holz, S. A. Hughes, N. Dalal, and J. L. Sievers, Exploring short gamma-ray bursts as gravitational-wave standard sirens, *Astrophys. J.* **725**, 496 (2010), [arXiv:0904.1017 \[astro-ph.CO\]](#).
- [13] P. Petrov, L. P. Singer, M. W. Coughlin, V. Kumar, M. Almualla, S. Anand, M. Bulla, T. Dietrich, F. Foucart, and N. Guessoum, Data-driven Expectations for Electromagnetic Counterpart Searches Based on LIGO/Virgo Public Alerts, *Astrophys. J.* **924**, 54 (2022), [arXiv:2108.07277 \[astro-ph.HE\]](#).
- [14] Q. Chu, E. J. Howell, A. Rowlinson, H. Gao, B. Zhang, S. J. Tingay, M. Boër, and L. Wen, Capturing the electromagnetic counterparts of binary neutron star mergers through low latency gravitational wave triggers, *Mon. Not. Roy. Astron. Soc.* **459**, 121 (2016), [arXiv:1509.06876 \[astro-ph.HE\]](#).
- [15] S. Ghosh, S. Bloemen, G. Nelemans, P. J. Groot, and L. R. Price, Tiling strategies for optical follow-up of gravitational-wave triggers by telescopes with a wide field of view, *Astron. Astrophys.* **592**, A82 (2016), [arXiv:1511.02673 \[astro-ph.IM\]](#).
- [16] M. W. Coughlin *et al.*, Optimizing searches for electromagnetic counterparts of gravitational wave triggers, *Mon. Not. Roy. Astron. Soc.* **478**, 692 (2018), [arXiv:1803.02255 \[astro-ph.IM\]](#).
- [17] K. Cannon *et al.*, Toward Early-Warning Detection of Gravitational Waves from Compact Binary Coalescence, *Astrophys. J.* **748**, 136 (2012), [arXiv:1107.2665 \[astro-ph.IM\]](#).
- [18] M. L. Chan, C. Messenger, I. S. Heng, and M. Hendry, Binary Neutron Star Mergers and Third Generation Detectors: Localization and Early Warning, *Phys. Rev. D* **97**, 123014 (2018), [arXiv:1803.09680 \[astro-ph.HE\]](#).
- [19] A. H. Nitz, M. Schäfer, and T. Dal Canton, Gravitational-wave Merger Forecasting: Scenarios for the Early Detection and Localization of Compact-binary Mergers with Ground-based Observatories, *Astrophys. J. Lett.* **902**, L29 (2020), [arXiv:2009.04439 \[astro-ph.HE\]](#).
- [20] M. K. Singh, S. J. Kapadia, M. A. Shaikh, D. Chatterjee, and P. Ajith, Improved early warning of compact binary mergers using higher modes of gravitational radiation: A population study, *Mon. Not. Roy. Astron. Soc.* **502**, 1612 (2021), [arXiv:2010.12407 \[astro-ph.HE\]](#).
- [21] T. Tsutsui, A. Nishizawa, and S. Morisaki, Early warning of precessing compact binary merger with third-generation gravitational-wave detectors, *Phys. Rev. D* **104**, 064013 (2021), [arXiv:2011.06130 \[gr-qc\]](#).
- [22] R. Magee *et al.*, First demonstration of early warning gravitational wave alerts, *Astrophys. J. Lett.* **910**, L21 (2021), [arXiv:2102.04555 \[astro-ph.HE\]](#).
- [23] T. Tsutsui, A. Nishizawa, and S. Morisaki, Early warning of precessing neutron-star black hole binary mergers with the near-future gravitational-wave detectors, *Mon. Not. Roy. Astron. Soc.* **512**, 3878 (2022), [arXiv:2107.12531 \[gr-qc\]](#).
- [24] C. Chatterjee and L. Wen, Pre-merger sky localization of gravitational waves from binary neutron star mergers using deep learning, (2022), [arXiv:2301.03558 \[astro-ph.HE\]](#).
- [25] Y. Li, I. S. Heng, M. L. Chan, C. Messenger, and X. Fan, Exploring the sky localization and early warning capabilities of third generation gravitational wave detectors in three-detector network configurations, *Phys. Rev. D* **105**, 043010 (2022), [arXiv:2109.07389 \[astro-ph.IM\]](#).
- [26] A. Nishizawa, E. Berti, A. Klein, and A. Sesana, eLISA eccentricity measurements as tracers of binary black hole formation, *Phys. Rev. D* **94**, 064020 (2016), [arXiv:1605.01341 \[gr-qc\]](#).
- [27] A. Nishizawa, A. Sesana, E. Berti, and A. Klein, Constraining stellar binary black hole formation scenarios with eLISA eccentricity measurements, *Mon. Not. Roy. Astron. Soc.* **465**, 4375 (2017), [arXiv:1606.09295 \[astro-ph.HE\]](#).
- [28] K. Breivik, C. L. Rodriguez, S. L. Larson, V. Kalogera, and F. A. Rasio, Distinguishing Between Formation Channels for Binary Black Holes with LISA, *Astrophys. J. Lett.* **830**, L18 (2016), [arXiv:1606.09558 \[astro-ph.GA\]](#).
- [29] M. Zevin, I. M. Romero-Shaw, K. Kremer, E. Thrane, and P. D. Lasky, Implications of Eccentric Observations on Binary Black Hole Formation Channels, *Astrophys. J. Lett.* **921**, L43 (2021), [arXiv:2106.09042 \[astro-ph.HE\]](#).
- [30] B. Sun, Z. Cao, Y. Wang, and H.-C. Yeh, Parameter estimation of eccentric inspiraling compact binaries using an enhanced post circular model for ground-based detectors, *Phys. Rev. D* **92**, 044034 (2015).
- [31] S. Ma, Z. Cao, C.-Y. Lin, H.-P. Pan, and H.-J. Yo, Gravitational wave source localization for eccentric binary coalescence with a ground-based detector network, *Phys. Rev. D* **96**, 084046 (2017), [arXiv:1710.02965 \[gr-qc\]](#).

- [32] H.-P. Pan, C.-Y. Lin, Z. Cao, and H.-J. Yo, Accuracy of source localization for eccentric inspiraling binary mergers using a ground-based detector network, *Phys. Rev. D* **100**, 124003 (2019), [arXiv:1912.04455 \[gr-qc\]](#).
- [33] B. Mikoczi, B. Kocsis, P. Forgacs, and M. Vasuth, Parameter estimation for inspiraling eccentric compact binaries including pericenter precession, *Phys. Rev. D* **86**, 104027 (2012), [arXiv:1206.5786 \[gr-qc\]](#).
- [34] K. Kyutoku and N. Seto, Pre-merger localization of eccentric compact binary coalescences with second-generation gravitational-wave detector networks, *Mon. Not. Roy. Astron. Soc.* **441**, 1934 (2014), [arXiv:1312.2953 \[astro-ph.HE\]](#).
- [35] T. Yang, R.-G. Cai, Z. Cao, and H. M. Lee, Eccentricity of Long Inspiring Compact Binaries Sheds Light on Dark Sirens, *Phys. Rev. Lett.* **129**, 191102 (2022), [arXiv:2202.08608 \[gr-qc\]](#).
- [36] T. Yang, R.-G. Cai, and H. M. Lee, Space-borne atom interferometric gravitational wave detections. Part III. Eccentricity on dark sirens, *JCAP* **10**, 061, [arXiv:2208.10998 \[gr-qc\]](#).
- [37] T. Yang, R.-G. Cai, Z. Cao, and H. M. Lee, Parameter estimation of eccentric gravitational waves with a decihertz observatory and its cosmological implications, *Phys. Rev. D* **107**, 043539 (2023), [arXiv:2212.11131 \[gr-qc\]](#).
- [38] M. Favata, Systematic parameter errors in inspiraling neutron star binaries, *Phys. Rev. Lett.* **112**, 101101 (2014), [arXiv:1310.8288 \[gr-qc\]](#).
- [39] M. Favata, C. Kim, K. G. Arun, J. Kim, and H. W. Lee, Constraining the orbital eccentricity of inspiralling compact binary systems with Advanced LIGO, *Phys. Rev. D* **105**, 023003 (2022), [arXiv:2108.05861 \[gr-qc\]](#).
- [40] H. Gil Choi, T. Yang, and H. M. Lee, Importance of Eccentricities in Parameter Estimation of Compact Binary Inspirals with Decihertz Gravitational-Wave Detectors, (2022), [arXiv:2210.09541 \[gr-qc\]](#).
- [41] I. M. Romero-Shaw, P. D. Lasky, E. Thrane, and J. C. Bustillo, GW190521: orbital eccentricity and signatures of dynamical formation in a binary black hole merger signal, *Astrophys. J. Lett.* **903**, L5 (2020), [arXiv:2009.04771 \[astro-ph.HE\]](#).
- [42] V. Gayathri, J. Healy, J. Lange, B. O'Brien, M. Szczepanczyk, I. Bartos, M. Campanelli, S. Klimentenko, C. O. Lousto, and R. O'Shaughnessy, Eccentricity estimate for black hole mergers with numerical relativity simulations, *Nature Astron.* **6**, 344 (2022), [arXiv:2009.05461 \[astro-ph.HE\]](#).
- [43] N. Yunes, K. G. Arun, E. Berti, and C. M. Will, Post-Circular Expansion of Eccentric Binary Inspirals: Fourier-Domain Waveforms in the Stationary Phase Approximation, *Phys. Rev. D* **80**, 084001 (2009), [Erratum: *Phys. Rev. D* **89**, 109901 (2014)], [arXiv:0906.0313 \[gr-qc\]](#).
- [44] E. A. Huerta, P. Kumar, S. T. McWilliams, R. O'Shaughnessy, and N. Yunes, Accurate and efficient waveforms for compact binaries on eccentric orbits, *Phys. Rev. D* **90**, 084016 (2014), [arXiv:1408.3406 \[gr-qc\]](#).
- [45] B. Moore, T. Robson, N. Loutrel, and N. Yunes, Towards a Fourier domain waveform for non-spinning binaries with arbitrary eccentricity, *Class. Quant. Grav.* **35**, 235006 (2018), [arXiv:1807.07163 \[gr-qc\]](#).
- [46] B. Moore and N. Yunes, A 3PN Fourier Domain Waveform for Non-Spinning Binaries with Moderate Eccentricity, *Class. Quant. Grav.* **36**, 185003 (2019), [arXiv:1903.05203 \[gr-qc\]](#).
- [47] D. Tsang, J. S. Read, T. Hinderer, A. L. Piro, and R. Bondarescu, Resonant Shattering of Neutron Star Crusts, *Phys. Rev. Lett.* **108**, 011102 (2012), [arXiv:1110.0467 \[astro-ph.HE\]](#).
- [48] A. G. Suvorov and K. D. Kokkotas, Precursor flares of short gamma-ray bursts from crust yielding due to tidal resonances in coalescing binaries of rotating, magnetized neutron stars, *Phys. Rev. D* **101**, 083002 (2020), [arXiv:2003.05673 \[astro-ph.HE\]](#).
- [49] M. Lyutikov, Electrodynamics of binary neutron star mergers, *Mon. Not. Roy. Astron. Soc.* **483**, 2766 (2019), [arXiv:1809.10478 \[astro-ph.HE\]](#).
- [50] V. Paschalidis, Z. B. Etienne, and S. L. Shapiro, General relativistic simulations of binary black hole-neutron stars: Precursor electromagnetic signals, *Phys. Rev. D* **88**, 021504 (2013), [arXiv:1304.1805 \[astro-ph.HE\]](#).
- [51] R. Abbott *et al.* (LIGO Scientific, VIRGO, KAGRA), GWTC-3: Compact Binary Coalescences Observed by LIGO and Virgo During the Second Part of the Third Observing Run, (2021), [arXiv:2111.03606 \[gr-qc\]](#).
- [52] M. Punturo *et al.*, The Einstein Telescope: A third-generation gravitational wave observatory, *Class. Quant. Grav.* **27**, 194002 (2010).
- [53] LIGO Scientific Collaboration, *LIGO Algorithm Library - LALSuite*, free software (GPL) (2018).
- [54] A. Nitz, I. Harry, D. Brown, C. M. Biwer, J. Willis, T. D. Canton, C. Capano, T. Dent, L. Pekowsky, A. R. Williamson, S. De, M. Cabero, B. Machenschalk, D. Macleod, P. Kumar, F. Pannarale, S. Reyes, G. S. C. Davies, dfinstad, S. Kumar, M. Tápai, L. Singer, S. Khan, S. Fairhurst, A. Nielsen, S. Singh, T. Massinger, K. Chandra, shasvath, and veronica villa, *gwastro/pycbc: v2.0.5 release of pycbc* (2022).
- [55] C. Cutler and E. E. Flanagan, Gravitational waves from merging compact binaries: How accurately can one extract the binary's parameters from the inspiral wave form?, *Phys. Rev. D* **49**, 2658 (1994), [arXiv:gr-qc/9402014](#).
- [56] C. Cutler, Angular resolution of the LISA gravitational wave detector, *Phys. Rev. D* **57**, 7089 (1998), [arXiv:gr-qc/9703068](#).
- [57] H.-S. Cho, Systematic bias due to eccentricity in parameter estimation for merging binary neutron stars, *Phys. Rev. D* **105**, 124022 (2022), [arXiv:2205.12531 \[gr-qc\]](#).
- [58] A. A. Abdo *et al.* (Fermi-LAT, Fermi GBM), Fermi Observations of High-Energy Gamma-Ray Emission from GRB 080916C, *Science* **323**, 1688 (2009).
- [59] E. Nakar, A. Gal-Yam, and D. B. Fox, The Local Rate and the Progenitor Lifetimes of Short-Hard Gamma-Ray Bursts: Synthesis and Predictions for LIGO, *Astrophys. J.* **650**, 281 (2006), [arXiv:astro-ph/0511254](#).
- [60] L. Rezzolla, B. Giacomazzo, L. Baiotti, J. Granot, C. Kouveliotou, and M. A. Aloy, The missing link: Merging neutron stars naturally produce jet-like structures and can power short Gamma-Ray Bursts, *Astrophys. J. Lett.* **732**, L6 (2011), [arXiv:1101.4298 \[astro-ph.HE\]](#).
- [61] K. P. Mooley, J. Anderson, and W. Lu, Optical superluminal motion measurement in the neutron-star merger GW170817, *Nature* **610**, 273 (2022), [arXiv:2210.06568 \[astro-ph.HE\]](#).
- [62] V. Connaughton *et al.*, Fermi GBM Observations of LIGO Gravitational Wave event GW150914, *Astrophys. J. Lett.* **826**, L6 (2016), [arXiv:1602.03920 \[astro-ph.HE\]](#).

- [63] A. Loeb, Electromagnetic Counterparts to Black Hole Mergers Detected by LIGO, *Astrophys. J. Lett.* **819**, L21 (2016), [arXiv:1602.04735 \[astro-ph.HE\]](#).
- [64] S. E. d. Mink and A. King, Electromagnetic signals following stellar-mass black hole mergers, *Astrophys. J. Lett.* **839**, L7 (2017), [arXiv:1703.07794 \[astro-ph.HE\]](#).